



# Increasing Quality Control of Ultrasonically Welded Joints Through Gaussian Process Regression

P. G. Mongan<sup>1,2</sup>(✉), E. P. Hinchy<sup>1,2</sup>, N. P. O'Dowd<sup>1,2,3</sup>, and C. T. McCarthy<sup>1,2,3</sup>

<sup>1</sup> Confirm Smart Manufacturing Research Centre, Limerick, Ireland  
patrick.mongan@ul.ie

<sup>2</sup> School of Engineering, University of Limerick, Limerick V94 T9PX, Ireland

<sup>3</sup> Bernal Institute, University of Limerick, Limerick V94 T9PX, Ireland

**Abstract.** Due to the recent advances in digitisation of the manufacturing industry and the generation of manufacturing data, there is increasing interest to integrate machine learning on the shop floor to improve efficiency and quality control. Ultrasonic welding is an emerging joining process used in various manufacturing industries, and is an energy efficient, cost-effective method of joining similar or dissimilar materials. However, the quality of the joint achievable is heavily dependent on process input parameters. In this study, a Gaussian Process Regression (GPR) model is developed to map the relationship between process parameters and joint performance for ultrasonically welded aluminium joints, with a view to improving quality control in a manufacturing setting. Initially, a 3<sup>3</sup> full factorial design of experiments is conducted to investigate the influential parameters, then a GPR model is trained on the experimental data. In-process sensor data is also used to infer process performance. To assess the prediction performance of the model, ten unseen parameter combinations are predicted and compared to their respective experimental result. The model demonstrates a high level of accuracy producing a Pearson's correlation coefficient of 0.982 between the predicted and actual results for all data. The mean relative predictive error for unseen data is 7.35%.

**Keywords:** Ultrasonic welding · Machine learning · Gaussian process regression · Quality control

## 1 Introduction

Joining is a critical step for the assembling of components in the manufacturing sector (e.g., there are typically 3000–4000 spot welds in an automobile body [1]) and joining of alloys in an active area of research. Joining is typically segregated into three categories: mechanical, thermal, and chemical. Regardless of the technique used, quality control is paramount as the joint is regularly the weak point where structural failure initiates. The recent trend towards the vision of the fourth industrial revolution promotes the use of

information technology in manufacturing [2]. Therefore, developing intelligent ways of exploiting information for process monitoring purposes is an active area of research.

Ultrasonic Welding (USW) is a prominent emerging technology, that is extensively used in industry due to its fast process times, low energy consumption, ease of automation and potential to become a smart manufacturing process. USW uses electrical energy to produce high frequency (10–70 kHz) low amplitude mechanical vibrations (10–250  $\mu\text{m}$ ), generating a relative motion between two mating surfaces [3]. In metal ultrasonic welding, this motion results in local plastic deformation and the shearing of the surface oxide layer, creating metal-to-metal contact and thus producing a solid-state bond [4]. Various researchers have investigated USW in a bid to optimise the process for their respective application while sharing insight into parameter relationships. Patel et al. [5] investigated the application of USW to join AZ31 magnesium alloy and stated welding energy is the most influential parameter. Nong et al. [6] examined the application of USW for the joining of lithium-ion battery cells, concluding USW yields quality results under optimal conditions.

In USW, process input parameters have a significant impact of the mechanical properties of the joint achieved [7, 8]. The complex relationship between input parameters and joint performance is key to optimising the process and predicting the joint performance under ideal process conditions. However, in manufacturing environments there is no guarantee that all processes are conducted under optimal conditions. This in turn can result in poor performing joints slipping through quality control. This study tackles the issue by incorporating process information into the model's prediction. Process information such as peak power, is real time system feedback that can account for unanticipated variabilities during the welding process, such as the presence of surface oil which can lead to poor joint quality [6].

USW is a convoluted process, therefore, requires a robust model to accurately predict joint performance. Various researchers have investigated the application of machine learning approaches to model the process. Li et al. [9] developed an Artificial Neural Network (ANN) to predict joint performance of USW composite joints. The model's inputs accounted for material processing parameters such as annealing temperature and surface condition, and process parameters such as welding energy, plunging speed and trigger force. Zhao et al. [10] created an ANN to capture the relationships between process parameters and joint performance for metal USW joints. The study highlighted the importance of considering multiple process parameters due to parameter interactions and also demonstrated the ability to create a robust model of the process. However, the above studies developed deterministic methods, which provide discrete predictions, but it is difficult to obtain information in relation to the prediction uncertainty. Stochastic methods such as Gaussian Process Regression (GPR) have the ability to predict the mean performance of the joint and provide the prediction standard deviation that can be used to define a 95% confidence window. The larger the confidence window the greater the uncertainty in the prediction. GPR is receiving significant attention in the machine learning domain and is being applied to various engineering problems [11]. GPR is a non-parametric technique capable of constructing a model for a complex system with noisy observations and uncertainties [12]. Cheng et al. [13], demonstrated the benefits of using a GPR model to accurately predict the surface residual stress in an end milling

application and produced a correlation coefficient of 0.9436 between predicted and actual results. Leco et al. [14], developed a GPR model for in-situ prediction of a robotic countersinking application, demonstrating a high level of accuracy in the predictions (error within  $\pm 0.2$  mm).

In this study, a GPR model is developed to predict the Lap Shear Strength (LSS), a measure of how much shear force a lap joint can withstand before failure occurs, of USW joints, with a view to improving quality control in a manufacturing setting. The prediction is formulated based on process input parameters and real time process feedback coming from integrated sensor data. The input parameters incorporated are welding energy, vibration amplitude and clamping pressure. Peak power is the maximum power required during the welding process and is included in the prediction to detect and quantify process variation. The GPR model developed in this study addresses the main drawback of using deterministic methods for quality predictions, which is no quantification of prediction uncertainty, by providing a probability distribution over possible predictions.

## 2 Machine Learning

This work exploits the experimental space by adjusting controllable variables to build and train a data driven model for joint quality prediction. Figure 1 represents a schematic of the supervised learning prediction approach implemented in this study. The data are collected from destructive testing. In manufacturing environments, destructive testing increases product waste, reduces efficiency, and only assess joints at predefined intervals. The proposed model has the potential to eliminate destructive testing while increasing quality control by predicting the performance of each welded joint.

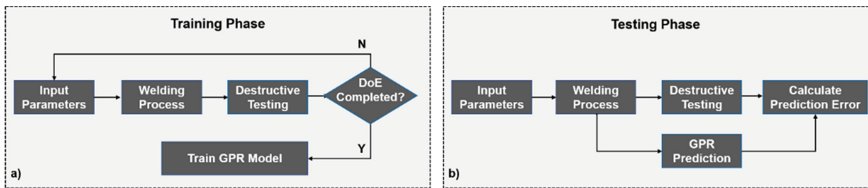


**Fig. 1.** Schematic of a) training phase and b) testing phase of the supervised learning approach.

### 2.1 Gaussian Process Regression

This study implements GPR to model the USW process. GPR was selected due to its ability to deal with uncertainty in a probabilistic framework. Therefore, models developed using GPR provide not only the best function for mapping input to output data, but also allows for a probability distribution over likely functions [15]. A brief overview of GPR is given in the following and is based on [12], where a detailed explanation of GPR can be found.

Given that  $X = \{(x_i, y_i) \mid i = 1, 2, \dots, N\}$  represents the training dataset, where  $x_i = (x_i^1, x_i^2, \dots, x_i^D)^T$  represents the  $i^{\text{th}}$  iteration of the  $D$ -dimensional input vector and  $y_i$  is

the corresponding output for  $x_i$ . Then the union of any finite Gaussian process (GP) can be fully specified by the mean function  $m(x)$  and a covariance function  $k(x, x')$  [16]. The GP is represented as follows:

$$f(x) \sim GP(m(x), k(x, x')) \tag{1}$$

where,

$$m(x) = E[f(x)] \tag{2}$$

$$k(x, x') = E[(f(x) - m(x))(f(x') - m(x')))] \tag{3}$$

where  $E[]$  is the expectation.

The objective of this work is to predict the LSS response ( $y_{N+1}$ ) when a vector ( $x_{N+1}$ ) containing process parameters and process feedback is provided. This study implements a zero mean function and because the kernel function is a key element of GP's, various kernel functions are explored [17]. The study investigated exponential (Eq. 4), squared exponential (SE) (Eq. 5), rational quadratic (RQ) (Eq. 6), and the Matérn (Eq. 7) kernels. The mathematical formulation of the kernels are as follows:

$$Exponential(x, x') = \exp\left(-\frac{|x - x'|}{l}\right) \tag{4}$$

where  $l$  is the correlation length parameter.

$$SE(x, x') = \exp\left(-\frac{|x - x'|^2}{2l^2}\right) \tag{5}$$

$$RQ(x, x') = \left(1 + \frac{|x - x'|^2}{2\alpha l^2}\right)^{-\alpha} \tag{6}$$

where  $\alpha$  is the relative weighing [18].

$$Matern(x, x') = \frac{1}{2^{\nu-1}\Gamma(\nu)} \left(\sqrt{2\nu}\frac{|x - x'|}{l}\right)^2 \mathcal{B}_\nu\left(\sqrt{2\nu}\frac{|x - x'|}{l}\right) \tag{7}$$

where  $\Gamma$  is the standard Gamma function,  $\mathcal{B}_\nu$  is the modified Bessel function, [19], and  $\nu$  is a hyperparameter that controls the smoothness of the resulting function. As  $\nu \rightarrow \infty$  the Matérn kernel becomes the SE kernel and when  $\nu = 0.5$  the Matérn kernel becomes the Exponential kernel.

## 2.2 Model Selection

This study analysed various GPR models consisting of different kernels with varying hyperparameters. To accurately compare the different models a holdout validation technique was employed. This meant three data samples were withheld from training

to evaluate the model’s ability to generalise. The models were assessed based on their mean absolute percentage error (MAPE) (Eq. 8) between the predicted and actual values for the validation dataset.

$$MAPE = \frac{1}{n} \sum \left( \frac{\text{actual value} - \text{predicted value}}{\text{predicted value}} \times 100 \right) \quad (8)$$

### 3 Experimental Procedure

The material used in this study is aluminium 5754, a commercial alloy typically used in automotive vehicle bodies. A schematic of the USW configuration and specimen dimensions is provided in Fig. 2. The welding process was performed using a Branson Ultraweld L20 ultrasonic welder equipped with a rectangular sonotrode with dimensions of  $18 \times 10 \text{ mm}^2$  and a 20 kHz power supply. Post-welding, the joint performance was assessed using a Tinius Olsen universal tester equipped with a 10 kN load cell at a crosshead velocity of 1 mm/min.

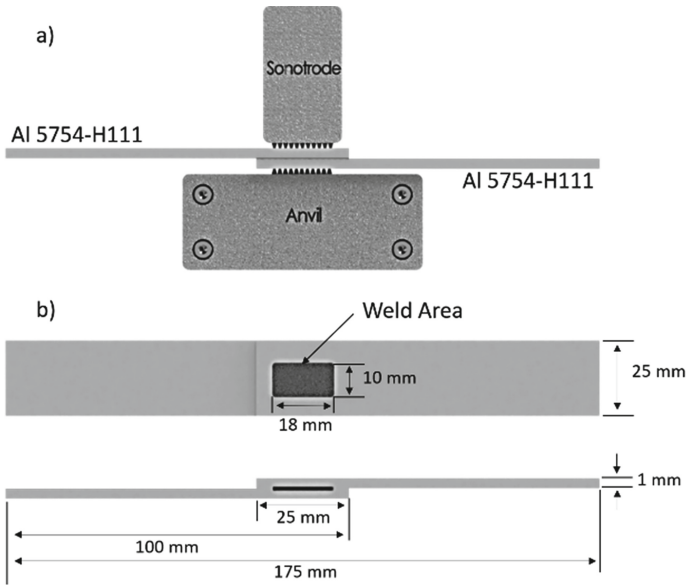


Fig. 2. Schematic of (a) welding configuration and (b) welded specimens.

The welding process was conducted on the energy control mode, which terminated the process when the joint interface absorbed the preselected energy. The parameter levels for the design of experiments (DoE) are outlined Table 1.

A large parameter range was selected for each of the variables to provide data to characterise the welding process over a large application field. Preliminary testing discovered that USW of the test alloy requires the following: a minimum energy of 700 J to achieve a bond; 3 kJ produces a satisfactory joint; a clamp pressure exceeding 0.45 MPa will result in no joint due to collapse and/or surface cracks.

**Table 1.** DoE parameters and levels

Parameter	Levels
Welding energy (kJ)	[10, 2.25, 3.5]
Vibration amplitude ( $\mu\text{m}$ )	[45, 55, 65]
Clamping pressure (MPa)	[0.2, 0.3, 0.4]

### 3.1 Experimental Data Analysis

Figure 3 shows the distribution of LSS for different welding energies obtained from the DoE. Welding energy is a strong contributor to LSS, indicated by the LSS response increasing across each graph. It is also evident that there are strong interactions between the input parameters as the relationship between clamping pressure and LSS changes with an increase in welding energy. Vibration amplitude is also a significant contributor to LSS outlined by the increase in LSS as a result of increasing the vibration amplitude, while additional input parameters remain fixed.

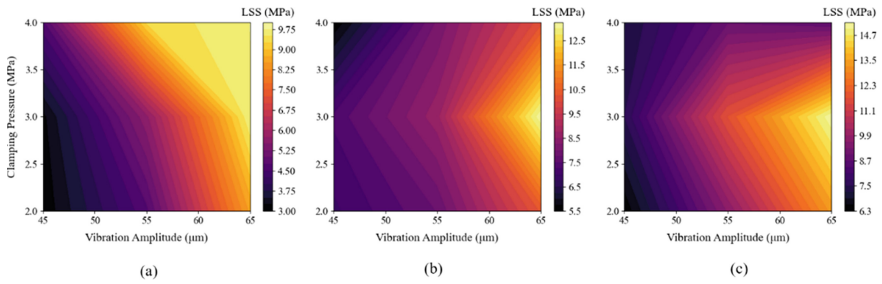


**Fig. 3.** Distribution of joint strength for different welding energies, welding energy = (a) 1.0 kJ, (b) 2.25 kJ, (c) 3.5 kJ

## 4 Results

Figure 4 presents a comparison between the prediction performance of the different kernels investigated. Each of the respective models used to formulate the predictions in Fig. 4 have optimal hyperparameters which were identified through the grid search analysis. Table 2 outlines the Pearson’s Correlation Coefficient (PCC) and the MAPE for each of the model’s prediction performances across training and validation data. It is evident from Fig. 4 and Table 2 that the Matérn kernel was found to provide the most accurate predictions on the validation data (experiments 27–30) indicated by the closest alignment to the experimental values for the validation dataset, and the lowest MAPE of 5.03.

**Table 2.** Evaluation of the prediction performance for each kernel trialed.

Kernel	PCC	Training MAPE	Validation MAPE
Exponential	0.992	4.581	14.120
SE	0.991	4.306	10.802
RQ	0.989	4.622	7.465
Matérn	0.991	4.336	5.030

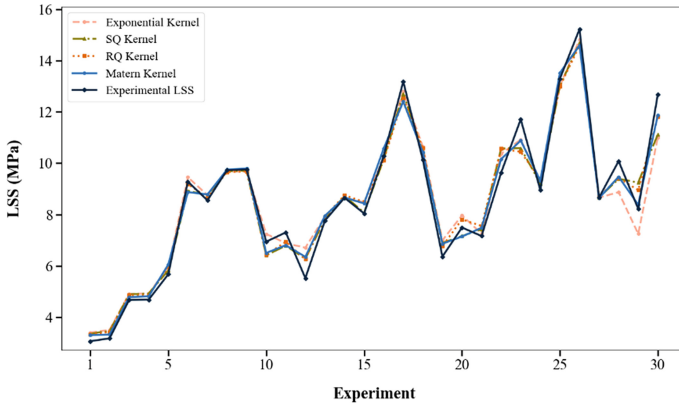


**Fig. 4.** Comparative analysis between the different kernels and the experimental result.

The corresponding  $l$  and  $\nu$  values for the kernel are [1, 2] and 0.75, respectively. There are four values for  $l$  to represent the correlation length parameter for each input into the GPR model (i.e., welding energy, vibration amplitude, clamping pressure, and peak power). Therefore, the following results outline the GPR model’s predictions using the Matérn kernel.

The optimal GPR model using the Matérn kernel was trained on twenty-seven experiments and validated on three experiments. A further seven experiments were conducted to evaluate the prediction performance on unseen data. The MAPE is 7.35 for all unseen data and 5.1 for all data. Table 3 and Fig. 5 highlight the predicted values and the prediction residual with the maximum residual being 1.22 and the maximum MAPE is 14.9.

Figure 5 (a) displays a regression analysis between the actual and predicted results for all data. The plot indicates a PCC of 0.982, indicating the strong relationship between the predicted and actual results. The plot also highlights error bars to indicate a 95% confidence interval in each prediction. Figure 5 (b) provides a comparative analysis between the actual and predicted values for the entire dataset. It is evident from the figure that the strong trend between predicted and actual values holds for all the data and the magnitude of the prediction error is low.

The GPR predictive model developed in this study demonstrates a high level of accuracy in predicting the performance of USW joints. It is evident from the prediction

residuals outlined in Table 3 that the magnitude of the residuals is similar throughout all data, indicating an accurately fit model. The GPR prediction is formulated based on process inputs and process feedback (integrated sensor data) therefore, the model can detect and predict unanticipated process variation. The approach can benefit manufacturing environments by increasing quality control by flagging anomalies in joint quality which can be used for rejecting parts. It is also noted, that although accurate, there are still variations in the prediction error. This is due to standard integrated sensors not being able to detect 100% of process variation [20]. Through ongoing research, the authors plan on addressing this issue through the inclusion of external sensing devices.

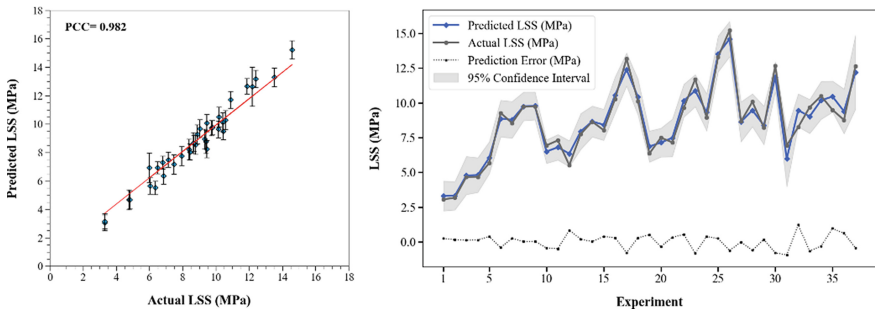


**Fig. 5.** Comparison between predicted and actual results. (a) regression analysis (b) comparative analysis indicating confidence interval and prediction error.

## 5 Conclusion

The main objective of this study was to develop a robust model to predict the performance of USW joints. The predictive model is based on GPR, where various kernels and hyperparameters were investigated. The study incorporated a holdout validation method to compare the respective models. The result of the grid search analysis found the Matérn kernel to be the most accurate. The predictions demonstrated a high level of accuracy with a correlation coefficient of 0.982 between the predicted and actual results. The *MAPE* for unseen data is 7.35.

The approach demonstrated in this study can be used in a manufacturing environment to provide in-situ performance predictions of welded joints that are fabricated using standard off the shelf welding equipment, thus minimising destructive testing. Such applications may include the joining of non-structural components for the automotive and aerospace industries. The predictions also outline a 95% confidence interval that can be used to quantify the model's prediction certainty. The GPR prediction can then be used to indicate if the welded joints are within control limits, thus increasing quality control. Through ongoing research, the authors are investigating methods of improving the prediction performance via the inclusion of additional sensing devices that provide further process insight in near real time.



**Acknowledgement.** This publication has emanated from research conducted in the Confirm Smart Manufacturing Research Centre, with the financial support of Science Foundation Ireland (SFI) under Grant Number SFI/16/RC/3918, co-funded by the European Regional Development Fund.

## Appendix

**Table 3.** Experimental results and predicted values.

Run number	Welding energy (J)	Vibration amplitude ( $\mu\text{m}$ )	Clamping pressure (MPa)	Peak power (W)	Actual LSS (MPa)	Predicted LSS (MPa)	Prediction residual (MPa)
1	1000	45	0.2	840	3.06	3.30	0.24
2	1000	45	0.3	880	3.17	3.32	0.15
3	1000	45	0.4	1160	4.67	4.78	0.11
4	1000	55	0.2	1060	4.68	4.81	0.13
5	1000	55	0.3	1200	5.67	6.05	0.38
6	1000	55	0.4	1440	9.28	8.87	-0.41
7	1000	65	0.2	1340	8.55	8.78	0.23
8	1000	65	0.3	1640	9.73	9.75	0.02
9	1000	65	0.4	1620	9.76	9.79	0.03
10	2250	45	0.2	820	6.94	6.50	-0.44
11	2250	45	0.3	860	7.30	6.80	-0.50
12	2250	45	0.4	800	5.52	6.35	0.83
13	2250	55	0.2	980	7.76	7.95	0.19
14	2250	55	0.3	1300	8.65	8.66	0.01
15	2250	55	0.4	1400	8.04	8.43	0.39
16	2250	65	0.2	1320	10.28	10.57	0.29
17	2250	65	0.3	1600	13.18	12.40	-0.78
18	2250	65	0.4	1800	10.13	10.42	0.29
19	3500	45	0.2	860	6.36	6.86	0.50
20	3500	45	0.3	920	7.49	7.14	-0.35
21	3500	45	0.4	1160	7.16	7.48	0.32
22	3500	55	0.2	1080	9.63	10.16	0.53
23	3500	55	0.3	1180	11.71	10.88	-0.83

(continued)

**Table 3.** (continued)

Run number	Welding energy (J)	Vibration amplitude ( $\mu\text{m}$ )	Clamping pressure (MPa)	Peak power (W)	Actual LSS (MPa)	Predicted LSS (MPa)	Prediction residual (MPa)
24	3500	55	0.4	1580	8.95	9.32	0.37
25	3500	65	0.2	1420	13.29	13.52	0.23
26	3500	65	0.3	1600	15.22	14.59	-0.63
27	3500	65	0.4	2560	8.66	8.64	-0.02
28	1500	60	0.35	1340	10.08	9.47	-0.61
29	3000	60	0.25	1960	8.22	8.38	0.16
30	3000	60	0.35	1560	12.67	11.87	-0.80
31	1500	50	0.3	1140	6.93	6.03	-0.90
32	1500	60	0.25	1340	8.25	9.47	1.22
33	2500	50	0.3	1020	9.69	9.03	-0.66
34	2500	60	0.25	1640	10.49	10.19	-0.30
35	2500	60	0.35	1580	9.49	10.46	0.97
36	3000	50	0.3	1060	8.77	9.40	0.63
37	4000	60	0.2	1360	12.63	12.20	-0.43

## References

1. Wang, X.: Vehicle noise and vibration refinement. Woodhead Publishing (2010)
2. Day, C.P.: Robotics in industry—their role in intelligent manufacturing. *Engineering* **4**(4), 440–445 (Aug. 01, 2018). <https://doi.org/10.1016/j.eng.2018.07.012>
3. Villegas, I.F.: Strength development versus process data in ultrasonic welding of thermo-plastic composites with flat energy directors and its application to the definition of optimum processing parameters. *Compos. A Appl. Sci. Manuf.* **65**, 27–37 (2014). <https://doi.org/10.1016/j.compositesa.2014.05.019>
4. Ni, Z.L.L., Ye, F.X.X.: Ultrasonic spot welding of aluminum alloys: A review. *J. Manuf. Process.* **35**(July), 580–594 (2018). <https://doi.org/10.1016/j.jmapro.2018.09.009>
5. Patel, V.K., Bhole, S.D., Chen, D.L., Patel, V.K., Bhole, S.D., Chen, D.L.: Ultrasonic spot welded AZ31 magnesium alloy: Microstructure, texture, and lap shear strength. *Mater. Sci. Eng., A* **569**, 78–85 (2013). <https://doi.org/10.1016/j.msea.2013.01.042>
6. Nong, L., Shao, C., Kim, T.H., Hu, S.J.: Improving process robustness in ultrasonic metal welding of lithium-ion batteries. *J. Manuf. Syst.* **48**, 45–54 (2018). <https://doi.org/10.1016/j.jmsy.2018.04.014>
7. Mongan, P.G., Hinchy, E.P., O’Dowd, N.P., McCarthy, C.T.: Optimisation of ultrasonically welded joints through machine learning. *Proc. CIRP* **93**, 527–531 (2020). <https://doi.org/10.1016/j.procir.2020.04.060>
8. Mongan, P.G., Hinchy, E.P., O’Dowd, N.P., McCarthy, C.T.: Quality prediction of ultrasonically welded joints using a hybrid machine learning model. *J. Manuf. Process.* **71**, 571–579 (2021). <https://doi.org/10.1016/J.JMAPRO.2021.09.044>

9. Li, Y., et al.: An artificial neural network model for predicting joint performance in ultrasonic welding of composites. *Proc. CIRP* **76**, 85–88 (2018). <https://doi.org/10.1016/j.procir.2018.01.010>
10. Zhao, D., Ren, D., Zhao, K., Pan, S., Guo, X.: Effect of welding parameters on tensile strength of ultrasonic spot welded joints of aluminum to steel—By experimentation and artificial neural network. *J. Manuf. Process.* **30**, 63–74 (2017). <https://doi.org/10.1016/j.jmapro.2017.08.009>
11. Lee, D.Y., Leifsson, L., Kim, J.Y., Lee, S.H.: Optimisation of hybrid tandem metal active gas welding using Gaussian process regression. *Sci. Technol. Weld. Joining* **25**(3), 208–217 (2020). <https://doi.org/10.1080/13621718.2019.1666222>
12. Rasmussen, C.E., Williams, C.: *Gaussian processes for machine learning* (2006)
13. Cheng, M., et al.: Prediction of surface residual stress in end milling with Gaussian process regression. *Meas. J. Int. Meas. Confederation* **178**, 109333 (Jun. 2021). <https://doi.org/10.1016/j.measurement.2021.109333>
14. Leco, M., Kadiramanathan, V.: A perturbation signal based data-driven Gaussian process regression model for in-process part quality prediction in robotic countersinking operations. *Robot. Comput. Integr. Manuf.* **71**, 102105 (2021). <https://doi.org/10.1016/j.rcim.2020.102105>
15. Snelson, E.: *Flexible and efficient Gaussian process models for machine learning* (2007)
16. Kong, D., Chen, Y., Li, N.: Gaussian process regression for tool wear prediction. *Mech. Syst. Signal Process.* **104**, 556–574 (2018). <https://doi.org/10.1016/j.ymsp.2017.11.021>
17. Mukesh Kumar, P.C., Kavitha, R.: Regression analysis for thermal properties of Al<sub>2</sub>O<sub>3</sub>/H<sub>2</sub>O nanofluid using machine learning techniques. *Heliyon* **6**(6), e03966 (Jun. 2020). <https://doi.org/10.1016/j.heliyon.2020.e03966>
18. Reggente, M., et al.: Prediction of ultrafine particle number concentrations in urban environments by means of Gaussian process regression based on measurements of oxides of nitrogen. *Environ. Model. Softw.* **61**, 135–150 (2014). <https://doi.org/10.1016/j.envsoft.2014.07.012>
19. Tolba, H., Dkhili, N., Nou, J., Eynard, J., Thil, S., Grieu, S.: GHI forecasting using Gaussian process regression: Kernel study. *IFAC-PapersOnLine* **52**(4), 455–460 (2019). <https://doi.org/10.1016/j.ifacol.2019.08.252>
20. Balz, I., et al.: Process monitoring of ultrasonic metal welding of battery tabs using external sensor data. *J. Adv. Joining Process.* **1**, 100005 (2020). <https://doi.org/10.1016/j.jajp.2020.100005>